



1 Validation of a new cavity ring-down spectrometer
2 for measuring tropospheric gaseous hydrogen
3 chloride

4 *Teles C. Furlani¹, Patrick R. Veres², Kathryn E.R. Dawe^{3, a}, J. Andrew Neuman^{2, 4}, Steven S.*
5 *Brown^{2, 5}, Trevor C. VandenBoer¹, Cora J. Young¹*

6 ¹ Department of Chemistry, York University, Toronto, ON, Canada

7 ² NOAA Chemical Sciences Laboratory, Boulder, CO, USA

8 ³ Department of Chemistry, Memorial University of Newfoundland, St. John's, NL, Canada

9 ⁴ Cooperative Institute for Research in Environmental Sciences, University of Colorado, Boulder, CO, USA

10 ⁵ Department of Chemistry, University of Colorado, Boulder, CO, USA

11 ^a Now at SEM Ltd., St. John's, NL, Canada

12 **Abstract**

13 Reliable, sensitive, and widely available hydrogen chloride (HCl) measurements are important for
14 understanding oxidation in many regions of the troposphere. We configured a commercial HCl
15 cavity ring-down spectrometer (CRDS) for sampling HCl in the ambient atmosphere and
16 developed calibration and validation techniques to characterize the measurement uncertainties.
17 The CRDS makes fast, sensitive, and robust measurements of HCl in a high finesse optical cavity
18 coupled to a laser centered at 5739 cm⁻¹. The accuracy was determined to reside between 5–10%,
19 calculated from laboratory calibrations and an ambient air intercomparison with annular denuders.
20 The precision and limit of detection (3σ) in the 0.5 Hz measurement were below 6 pptv and 18



21 pptv, respectively for a 30 second integration interval in zero air. The response time of this method
22 is primarily characterized by fitting decay curves to a double exponential equation and is impacted
23 by inlet adsorption/desorption, with these surface effects increasing with RH and decreasing with
24 decreasing HCl mixing ratios. The response time for the tested inlet was 2–6 minutes under the
25 most and least optimal conditions, respectively. An intercomparison with the EPA compendium
26 method for quantification of acidic atmospheric gases showed good agreement, yielding a linear
27 relationship statistically equivalent to unity (slope of 0.97 ± 0.15). The CRDS from this study can
28 detect HCl at atmospherically relevant mixing ratios, often performing comparable or better in
29 sensitivity, selectivity, and response-time from previously reported HCl detection methods.

30

31 **1. Introduction**

32 Halogenated compounds that participate in catalytic cycles in the atmosphere have major
33 impacts on atmospheric chemistry. Chlorine-containing species have long been known to
34 catalytically destroy stratospheric ozone (Solomon, 1999) and can have similar impacts on
35 tropospheric ozone in polar regions (Simpson et al., 2007, 2015). In particular, early morning
36 oxidation in the troposphere can be influenced heavily by chlorine atoms released by photolabile
37 chlorine species (Osthoff et al., 2008; Thornton et al., 2010; Young et al., 2012, 2014). It is
38 estimated that reactions involving chlorine atoms account for 14–27% of global tropospheric
39 oxidation of abundant volatile organic compounds (VOCs) (Sherwen et al., 2016).

40 The role of chlorine chemistry in the troposphere remains uncertain in part due to a lack of
41 a complete understanding of the contribution of chlorine reservoir species to the tropospheric
42 chlorine inventory (Osthoff et al., 2008; Young et al., 2014). Sources of inorganic chlorine to the
43 troposphere are important because many of them are photochemically active (e.g. ClNO₂). A near-

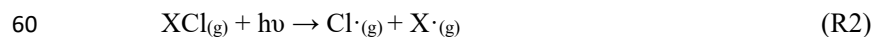


44 complete budget of inorganic tropospheric chlorine from aircraft transects of polluted North
45 American continental outflow during the WINTER campaign demonstrated that hydrogen chloride
46 (HCl) makes up 48–62 % of total inorganic chlorine, and approximately 98% of total gaseous
47 inorganic chlorine (Haskins et al., 2018). Troposphere HCl levels are typically between 10 and
48 1000 parts per trillion by volume (pptv) (e.g. Crisp et al. (2014); Haskins et al. (2018); and Young
49 et al. (2013)).

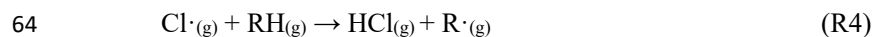
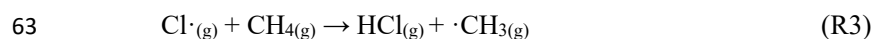
50 HCl is directly emitted to the atmosphere predominantly from volcanic activity, biomass
51 burning, and industrial sources (Butz et al., 2017; Crisp et al., 2014; Keene et al., 1999). HCl is
52 also produced through heterogeneous acid displacement reactions of strong acids, such as nitric
53 acid, with particulate chloride (pCl⁻) (Bondy et al., 2017; Clegg and Brimblecombe, 1985; Gard et
54 al., 1998; Valach, 1967; Wang et al., 2019):



56 where M represents a cation in a chloride salt (often sodium). Elevated levels of chlorine atoms
57 may also be present in both indoor and outdoor environments due to the emission of photolabile
58 reactive chlorine compounds (Dawe et al., 2019; Mattila et al., 2020; Osthoff et al., 2008; Young
59 et al., 2014, 2019).

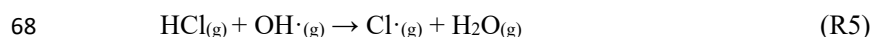


61 Secondary production of HCl predominantly occurs *via* the reaction of chlorine atoms with
62 methane or VOCs by hydrogen abstraction:





65 The loss of gas-phase HCl occurs predominantly through wet or dry deposition which are terminal
66 sinks for tropospheric chlorine (Wang et al., 2019), with minor loss by reaction with the hydroxyl
67 radical (OH) to re-form chlorine atoms:



69 The balance between loss and formation of chlorine atoms from HCl is highly dependent on factors
70 such as the presence of pCl⁻, NO_x (NO_x=NO+NO₂), and HCl deposition rate (Finlayson-Pitts et
71 al., 1989; Roberts et al., 2008).

72 Measuring HCl in the gas phase is challenging as it readily adsorbs to surfaces. Methods
73 for atmospheric HCl detection must be sensitive, robust, and selective and address HCl interactions
74 with instrument surfaces. Mass spectrometry based measurement techniques have been developed
75 for the detection of HCl in both the stratosphere and troposphere (e.g. Huey et al. (1996) and Marcy
76 et al. (2004)). Other methods include scrubbing ambient air using an annular denuder and/or a
77 tandem mist chambers to collect HCl, followed by offline analysis such as ion chromatography
78 (IC) (Keene et al., 2007, 2009; United States Environmental Protection Agency, 1999; Young et
79 al., 2013). Online detection methods such as chemical ionization time of flight mass spectrometry
80 (CI-ToF-MS) (Crisp et al., 2014), negative ion proton transfer chemical ionization mass
81 spectrometry (NI-PT-CIMS) (Veres et al., 2008), and negative mode atmospheric pressure
82 chemical ionization coupled to triple quadrupole mass spectrometry (APCI-MS-MS) (Karellas et
83 al., 2003) have been shown to be reliable and sensitive methods for HCl detection. Limitations to
84 these existing HCl measurement techniques include some or all of the following; detection limits
85 that are not suitable for the low level of HCl in the troposphere, slow time response, lack of
86 portability, and calibration challenges.



87 Measurements of HCl are typically calibrated using HCl from permeation devices and or
88 standards in compressed gas cylinders. Method validation for HCl measurements are rare, but can
89 reduce these uncertainties (Hagen et al., 2014). In this paper we demonstrate the versatility and
90 validation of a new commercial cavity ring-down spectrometer (CRDS) for in-situ atmospheric
91 gas phase HCl measurements. We compare this CRDS with existing HCl measurement techniques
92 through lab and field intercomparisons. Finally, we describe and characterize surface effects and
93 recommend inlet configurations for best practices when conducting ambient sampling.

94 **2. Materials and experimental methods**

95 **2.1 Chemicals**

96 Reagent grade hydrochloric acid (HCl, 12 M) was used in permeation device construction
97 (see Section 2.3). Potassium hydroxide (KOH) pellets were used to create scrubbing solution for
98 permeation device gas collection. Commercially available reagents were from Sigma-Aldrich
99 (Oakville, Ontario, Canada) and Ultra zero air (grade 5.0) gases were from Praxair (Toronto,
100 Ontario, Canada). Experiments used deionized water generated by a Barnstead Infinity Ultrapure
101 Water System (Thermo Fisher Scientific, Waltham, Massachusetts, USA; $18.2 \text{ M}\Omega \text{ cm}^{-1}$). Annular
102 denuder coating solution was prepared with reagent grade (>95.5%) sodium carbonate (Sigma-
103 Aldrich, St. Louis, Missouri, USA), reagent grade glycerol (Sigma-Aldrich, St. Louis, Missouri,
104 USA), HPLC grade methanol (Fisher Chemicals, Ottawa, Ontario, Canada), and $18.2 \text{ M}\Omega \text{ cm}^{-1}$
105 deionized water. Eluent for annular denuder IC analysis was prepared from sodium hydroxide
106 solution (NaOH, 50% w/w, Thermo Fisher Scientific, Sunnyvale, California, USA). IC calibration
107 standards were prepared through serial dilution of a mixed anion standard concentrate (Thermo
108 Fisher Scientific, Dionex Seven-Anion II, P/N: 057590). Nitrogen (grade 4.8).

109 **2.2. Cavity ring-down spectrometer (CRDS)**



110 The Picarro G2108 Hydrogen Chloride Gas Analyzer system was used for all analyses
111 (Dawe et al., 2019, www.picarro.com). The basic operating principles of this CRDS are similar to
112 analogous Picarro greenhouse gas instruments that have been described in detail by Crosson et. al
113 (2008). The CRDS consists of a tunable laser, a wavelength monitor, and a heated optical cavity
114 (80 °C). All the components of this analyzer and internal stainless-steel fittings are contained
115 within a heat-regulated metal case maintained at 45 °C. The laser radiation (1742 nm, 5739 cm⁻¹)
116 is directed by a fiber optic cable to the wavelength monitor and optical cavity. The first overtone
117 (2-0 absorption band) of HCl is easily discernable from other absorbing species (e.g. H₂O, CH₄),
118 has a relatively high intensity, and is accessible to near-infrared (IR) diode laser light sources. The
119 optical cavity is fitted with three highly reflective dielectric-coated fused silica mirrors (R >
120 99.995%, ring down time constant of 53 μsec, equivalent to a path length of 16 km) oriented in an
121 acute triangular arrangement supported by an invar housing. The reflectivity of the mirrors is
122 measured from the laser signal loss in an analyte-free optical cavity under inert gas flow. The
123 CRDS flow rate is 2 L min⁻¹ and the cavity is held at a reduced pressure of 18.70 ± 0.02 kPa (140
124 Torr) thermostated to 80.000 ± 0.005°C. One mirror is mounted on a piezoelectric actuator to
125 achieve optical resonance between the laser frequency and the longitudinal modes of the cavity.
126 The laser is shut off rapidly (< 1 μsec) once resonance is achieved. A photodetector monitors the
127 decay of the photons exiting the cavity through another mirror. Custom electronics digitize the
128 signal for fitting of an exponential decay; the time constant of the decay, τ, is converted to
129 absorbance, α, using the expression

130
$$\alpha = 1 / c\tau - 1 / c\tau_0 \quad E1$$

131 where c is the speed of light. The instrument measures 30 specific frequencies within ~1 cm⁻¹
132 centered at 5739 cm⁻¹ to fit the absorption spectra of trace species in this region (see Figure S1).



133 HCl, H₂O, and CH₄ mixing ratios are reported every 2 seconds, though the true time response of
134 the measurement method is limited by surface effects (see Section 3.4). Gaseous inorganic chlorine
135 reservoir species (e.g. ClNO₂) cannot thermally dissociated under the cavity (80 °C) conditions
136 (Thaler et al., 2011). The instrument zero measurement drift is reduced by a high precision
137 distributed feedback laser centered at 5739.2625 cm⁻¹ coupled with a custom-designed wavelength
138 monitor to determine the frequency axis of each spectrogram. To mitigate particulate matter optical
139 extinction and surface deposition on the high reflectivity mirrors, two high efficiency particulate
140 air (HEPA) filters are placed upstream of the cavity, contained within the 45 °C heat-regulated
141 compartment.

142 **2.3 In-house HCl permeation device validation**

143 The in-house assembly of HCl permeation devices (PDs) is described in detail in Lao et al.
144 (2020). Briefly, 200 μL of 12 M aqueous HCl solution was pipetted into a 7.62 cm perfluoroalkoxy
145 (PFA) tube (3 mm i.d. with 1 mm thickness) plugged at both ends with porous
146 polytetrafluoroethylene (PTFE) (1 cm length by 3.17 mm o.d.). The polymers allow a consistent
147 mass of HCl to permeate at a given temperature and pressure. An aluminum block that was
148 temperature-controlled using a cartridge heater (OmegaTM; CIR-2081/120V, Saint-Eustache, QC,
149 Canada) housed the PD and was regulated to 60.0 ± 0.1 °C by a process controller. Dry N₂ flowed
150 through a PFA tube (1.27 cm o.d.) in the block, containing the PD. Stable flows of 49 ± 2 standard
151 cubic centimeters per minute (sccm) through the oven were maintained with a 50 μm diameter
152 critical orifice (Lenox laser, Glen Arm, Maryland, USA, 15 psi; SS-4-VCR-2-50). Flows were
153 measured using a DryCal Definer 220 (Mesa Labs, Lakewood, Colorado, USA). The mass
154 emission rate of HCl from the PD was quantified by scrubbing into a 25 mL glass impinger



155 containing 1 mM KOH over 24 h followed by analysis using IC with conductivity detection (CD).
156 Mass emission rates for the PD were determined as $140 \pm 18 \text{ ng min}^{-1}$ ($n=3, \pm 1\sigma$) at $60 \text{ }^\circ\text{C}$.

157 **2.4 Laboratory intercomparison**

158 A laboratory intercomparison between the CRDS and offline-measured HCl scrubbed into
159 a basic solution of 100 mM KOH by delivering gaseous HCl from the permeation device to the
160 sampling systems. The 140 ng min^{-1} of HCl in dry N_2 from the PD was mixed into a zero air
161 dilution flow of 2.1 to 8.0 L min^{-1} , to provide standard addition HCl calibrations that ranged from
162 12 to 45 ppbv.

163 The dilution flow was maintained using a 10 L min^{-1} mass flow controller (GM50A, MKS
164 instruments, Andover, Massachusetts, USA). All inlet lines and fittings were kept at ambient
165 temperature ($\sim 25 \text{ }^\circ\text{C}$) and were made of PFA unless stated otherwise. The inlet mixing line
166 between the PD emissions and the humidified dilution flow was 3.17 mm i.d. and 45 cm in length.
167 Residence times for HCl in the sampling line ranged from 0.02 to 0.08 seconds. To vary relative
168 humidity (RH), a controlled flow of zero air was directed into a glass impinger at room temperature
169 containing deionized water to yield a water-saturated air stream. The humidified flow was passed
170 through a $2 \text{ }\mu\text{m}$ Teflon filter (TISCH scientific, North Bend, Ohio, USA) in a PFA holder to
171 prevent any aqueous droplets from entering the experimental lines. The RH was set by mixing
172 with dry zero air to generate 0, 20, 50, and 80 % RH values.

173 **2.5 Ambient intercomparison**

174 An ambient intercomparison was undertaken by measuring outdoor air with the CRDS in
175 parallel with sodium carbonate-coated annular denuders. A total of 11 denuder samples were
176 collected alongside continuous CRDS observations, each for approximately 24 hours between 4–
177 11 April 2019. The measurement site was the Air Quality Research Station, located on the roof of



178 the Petrie Science and Engineering Building at York University in Toronto, Ontario, Canada
179 (43.7738° N, 79.5071° W, 220 m above sea level). All indoor inlet lines and fittings were kept at
180 room temperature while the outdoor temperature ranged from -2 to 14 °C. All inlet lines and
181 fittings were made of PFA unless stated otherwise. A full schematic of the sampling apparatus
182 indicating the separation between the outdoor and indoor inlet positions is provided in Figure S4.
183 A 22 L min⁻¹ sampling flow was pulled through a URG Teflon Coated Aluminum Cyclone (URG
184 Corporation, Chapel Hill, North Carolina, USA) with a 2.5 µm cut-off for particulate matter. The
185 inlet lines were such that each sampling setup collected HCl at equal residence time to ensure
186 equivalent wall losses of HCl. The shared inlet line was 4.65 m in length and had an i.d. of 4.76
187 mm. The flow was split between the 1.5 m denuder sampling line (20 L min⁻¹) and the 0.15 m
188 CRDS sampling line (2 L min⁻¹), yielding a 0.375 sec residence time for both methods. The
189 denuder line flow was equally divided into two multichannel etched glass annular denuders (URG
190 Corporation, Chapel Hill, North Carolina, USA, 4 channel, 242 mm length, URG-2000-30x242-
191 4CSS) at 10 L min⁻¹. The denuders collected HCl in parallel to each other with flows controlled
192 using two separate 10 L min⁻¹ mass flow controllers (GM50A, MKS instruments). Denuders were
193 coated with a solution of 2% w/w sodium carbonate and 0.1% w/w glycerol in a solution of 1:1
194 methanol:water. A 15 mL aliquot of coating solution was dispensed into a denuder and two
195 polypropylene caps affixed. The sealed denuders were inverted and rotated for a few minutes to
196 ensure an even coating. The excess coating solution was decanted, and the denuder was dried for
197 15 min with 2 L min⁻¹ of zero air. After sampling, denuders were extracted with 2 aliquots of 5.00
198 mL deionized water, following the same sealing and inversion procedure, for a total extraction
199 volume of 10.00 mL. Extracts were collected into a 15 mL polypropylene tube for storage at 4 °C
200 until analysis. Instances of flagged instrument errors in the CRDS data during ambient



201 observations were removed as standard practice in quality control procedures (see Figure S2). The
202 loss of observational data during such periods corresponds to a negative bias. The CRDS data loss
203 during a given denuder sampling period was included in setting the overall measurement error
204 when intercomparing measurements.

205 **2.6 Ion chromatography analysis**

206 Samples collected into an impinger from the HCl PD were analyzed as the chloride anion
207 by IC-CD using an ICS-2100 (Thermo Fisher Scientific, Sunnyvale, California, USA) according
208 to the method described in Place et al. (2018). Annular denuder extracts were analyzed by IC-CD
209 using an ICS-6000 (Thermo Fisher Scientific, Sunnyvale, California, USA). Details of both
210 separation methods can be found in the SI. Chloride was quantified using external calibration with
211 a 5-point calibration curve. Two check standards, located at the high and low ends of the working
212 range, were used to evaluate the accuracy of quantification.

213 **3. Results and discussion**

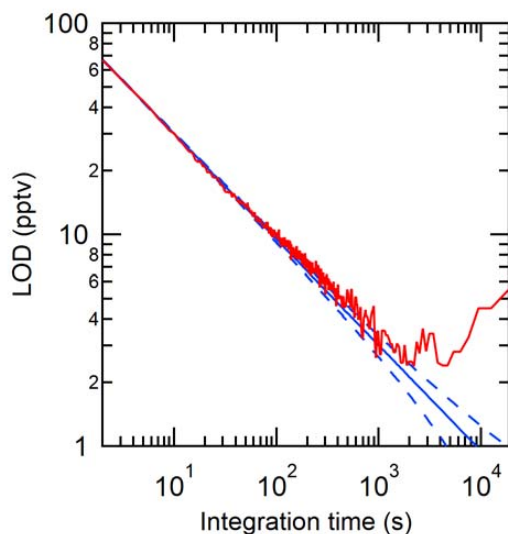
214 **3.1 Suitability for atmospheric measurements**

215 The selectivity of this CRDS analyzer arises from monitoring a high-intensity spectral line
216 (5739.2625 cm^{-1}). The absorption used by this instrument is suitable for HCl measurements in the
217 ambient atmosphere because abundant atmospheric gaseous species such as CO, CO₂, NO_x, and
218 N₂O (Gordon et al., 2017; Kochanov et al., 2019) do not have major absorption features in the
219 same region. Absorption features of H₂O and CH₄ in this spectral region are part of the fitting
220 parameters used to determine number densities of HCl, as described in Section 2.2. Most organic
221 and inorganic compounds commonly found at trace levels in the atmosphere do not absorb strongly
222 in this region (Gordon et al., 2017; Kochanov et al., 2019). For these compounds to interfere with
223 the CRDS measurement, their mixing ratios would need to be very high (>10s of parts per million



224 by volume, ppmv). Under conditions where the peak shape is compromised by the presence of
225 interfering absorbing species or instrument instabilities (e.g. cavity pressure fluctuations), the
226 instrument fitting is interrupted and the “bad” data is flagged, thereby allowing simple quality
227 control (see Figure S2).

228 The limit of detection (LOD) of the CRDS analyzer is suitable for expected HCl levels in
229 the atmosphere. Instrument LODs were calculated as three times the Allan-Werle deviation (Figure
230 1) when overflowing a 15 cm inlet (3.17 mm i.d.) with zero air directed into the CRDS for ~10
231 hours. The LODs determined in the CRDS measurements for 2 second, 30 second, and 1 hour
232 integration times were 95, 18, and 2 pptv, respectively. Similarly, precision was determined from
233 the Allan-Werle deviation in the blank over the same 10 hours of zero air sampling. Precision in a
234 2 second, 30 second, and 1 hour integration time was 32, 6, and 0.8 pptv, respectively.



235

236 **Figure 1.** Allan-Werle deviation (3σ) in the optical cavity purged with zero-air (red line) shown with the
237 ideal deviation (no drift, solid blue line) and associated error in the deviation (dashed blue line).

238



239 **3.2 Instrument performance**

240 The CRDS has many advantages compared to methods previously used to measure HCl in
241 the ambient atmosphere (Table 1). The LOD and precision of the instrument is comparable to prior
242 high time-resolution methods, allowing changes in HCl mixing ratio of a few pptv to be measured.
243 The accuracy/uncertainty is the hardest to compare due to the differences in assessment. A
244 particular challenge is that other methods require external calibrations to determine accuracy and
245 a stable, accurately calibrated HCl source at atmospherically relevant mixing ratios is challenging
246 to obtain (Lao et al., 2020; MacInnis et al., 2016). In contrast, spectroscopic techniques offer a
247 distinct advantage as they are absolute measurements and accuracy determinations rely on
248 propagating uncertainty in the measured parameters (i.e. wavelength and the time constant τ). In
249 the absence of determining accuracy of the CRDS from its operating parameters we use the
250 deviations in our intercomparisons to estimate the accuracy of the full system, i.e. the instrument
251 and ambient sampling inlet combined. We measured that the accuracy of the analyzer ranges from
252 5 to 15%. This is a conservative range based on the methods we used to validate the instrument,
253 which is further described in Section 3.3. The response time of the CRDS used in this work is fast
254 compared to most measurements; the limitation for all online-line methods compared in Table 1
255 is not the measurement frequency, but rather the time required for HCl to adsorb and desorb from
256 the inlet to the sample stream, which is discussed further in Section 3.5. Lastly, instrument size
257 and power consumption of this CRDS are much lower than many other techniques and are major
258 advantages when considering use in the field, particularly for mobile platforms.

259

260



261 **Table 1.** Performance characteristics of CRDS HCl analyzer compared to previously reported
 262 methods.

Instrument	LOD	Accuracy/ Uncertainty	Precision	Measurement frequency	Instrument Size	Power Consumption	Reference
<i>Near-IR CRDS</i>	<18 pptv ^a (30 sec)	5–15%	6 pptv (30 sec)	2 s ^e	31.75 kg 43.2 x 17.9 x 44.6 cm	110 W (analyzer) 75 W (pump)	This study
<i>Near-IR CRDS</i>	60 pptv ^a (1 min)	>10%	20 pptv (1 min)	<15 s	NR	NR	(Hagen et al., 2014)
<i>Aircraft laser infrared absorption spectrometer</i>	33 pptv ^b	10 %	0.1 ppbv (30 sec)	<30 s	72 kg	NR	(Voss et al., 2001; Webster et al., 1994)
<i>Quartz- enhanced photoacoustic spectroscopy (QEPAS)</i>	550 ppbv ^a	NR	526 ppbv	NR	NR	NR	(Ma et al., 2016)
<i>Acetate CI- ToF-MS</i>	97 pptv ^a	30%	32.3 pptv	<1 s	59 x 42 x 83 cm	<2000 W peak	(Crisp et al., 2014)
<i>Iodide CI- HR-ToF-MS</i>	30 pptv ^a (30 sec)	30%	53.3 pptv	0.22 s	~ 59 x 42 x 83 cm	<2000 W peak	(Lee et al., 2018)
<i>Sulfur pentafluoride ion trap CIMS</i>	66 pptv ^a	10%	22 pptv	1.6 s	NR	NR	(Jurkat et al., 2010)
<i>APCI-MS-MS</i>	335 pptv ^a	NR	NR	5 s	NR	< 17.5 kW	(Karellas et al., 2003)
<i>Tandem mist chamber and IC-CD</i>	48 pptv ^c	>25 %	24 pptv ^c	2 h	NR	NR	(Keene et al., 2007, 2009)
<i>Annular denuder and IC-CD</i>	6.9–42 pptv ^d	10%	NR	Hours–Days	>10 kg	400 W (sampling equipment only)	This study

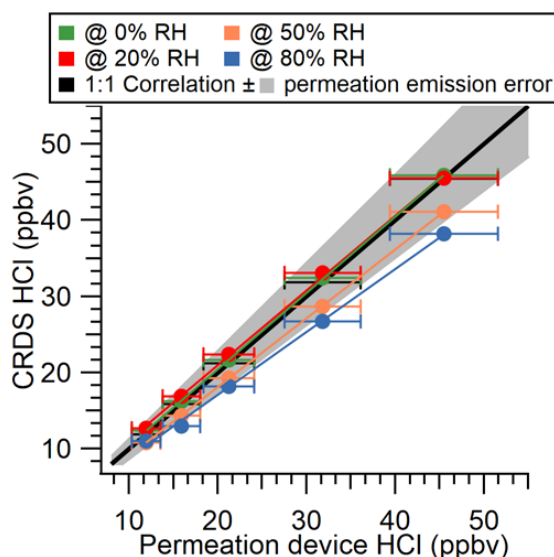
263 a: 3σ , b: predicted assuming a minimum detectable line-center absorption of 1×10^{-5} can be achieved in 30 s, c:

264 precision (σ) determined from averaged paired measurements in 2 h samples on IC-CD and LOD was calculated at



265 2σ , d: 3σ calculated range for a 24-hour sampling time from three denuder method blanks, e: instrument data reporting
266 frequency. The true measurement frequency will also be affected by surface effects, as described in section 3.4, and
267 NR: not reported.

268 3.3 Laboratory and ambient intercomparison



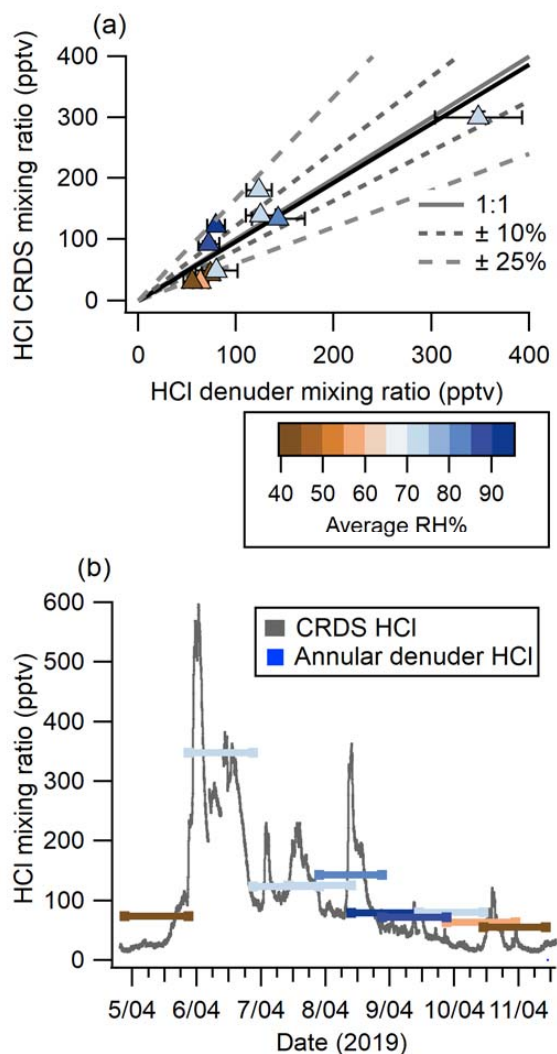
269

270 **Figure 2.** Comparison of CRDS HCl measurements and output from an HCl permeation device over a
271 range of RHs. Error bars in the x direction represent propagated IC measurement error, while error bars in
272 the y direction represent the standard deviation of online sampling plateau for each mixing ratio (low
273 magnitudes mean these error bars do not extend beyond the points). A 1:1 correlation (solid black line) is
274 shown with the uncertainty in the permeation device emission rate (shaded grey area).

275 We compared the CRDS analyzer-measured HCl with the gas standard mixing ratios
276 provided by an IC-certified PD under dry conditions and observed a close to 1:1 correlation (Figure
277 2). When the calibration gas entrained in flows of higher RH ($\geq 50\%$) a negative bias was
278 observed, although the measurements generally remained within the quantified error in the PD
279 output. Negative bias from the provided HCl mixing ratios at 50% and 80% RH were 9.6% and
280 14.9%, respectively. As described above, there is no spectroscopic water absorption interference
281 in the HCl measurement indicating that water increased HCl losses to gas handling surfaces for



282 experiments conducted in humidified air. Inlet surface effects are well established for gaseous
283 strong acids and bases, as these compounds readily sorb at interfaces (e.g. Eisele and Tanner
284 (1993), Kim et al. (2008), Neuman et al. (1999), Pszenny et al. (1993), Roscioli et al. (2016)). The
285 comparison presented here is a best-case scenario because the sampled mixing ratios were much
286 greater than expected in the ambient atmosphere, and therefore less likely to be impacted by
287 surface effects. Surface effects under humid conditions necessitated the mitigation and
288 quantification efforts described further in Section 3.5. To practically validate the CRDS under real-
289 world conditions, an ambient intercomparison was performed over a period of 7 days (4–11 April
290 2019).



291

292 **Figure 3.** (a) Comparison of HCl measured 4–11 April 2019 using annular denuders and CRDS (averaged
293 to the collection time of denuders). Denuder error bars are derived from the error in the IC calibration,
294 standard deviation of method blanks, and extraction recovery. CRDS measurement errors are the precision
295 in a single measurement combined with data loss for flagged instrument errors. Also shown are a 1:1
296 correlation line (solid grey), 10 % (short grey dash) and 25 % (long grey dash) deviation from 1:1, and the
297 orthogonal distance regression (solid black). Points are coloured by the average RH during sampling. (b)
298 Continuous HCl mixing ratio timeseries by CRDS overlaid with averaged 24-hour denuder measurement
299 analyzed by IC with lines coloured according to the average RH during sampling.



300

301 Online HCl detection by CRDS showed good agreement with HCl mixing ratios quantified
302 from ten annular denuder extracts collected according to EPA Compendium method IO-4.2
303 (United States Environmental Protection Agency, 1999), which is a standard offline method for
304 quantitation of acidic atmospheric gases (Figure 2a). Measurements from the 2 instruments were
305 linearly related with a slope of 0.97 ± 0.15 , as determined by orthogonal least distance regression,
306 with a y-intercept of -0.001 ± 0.021 . Half of the measurements are within 10 % of a 1:1 correlation
307 and the remaining half fall within 25 %. To further validate the comparison a linear correlation
308 coefficient (see Figure SI4) of 0.93 ± 0.14 was determined for the two methods and shows good
309 agreement with the orthogonal least distance regression. Changes in RH had no systematic bias
310 on the correlation. Our intercomparison indicates that CRDS measures HCl with comparable
311 results to those obtained by carbonate-coated annular denuders. While the latter requires offline
312 analysis, the CRDS has the additional benefit of continuous high time resolution measurements at
313 0.5 Hz and dramatically better precision.

314 Although average HCl measurements between the CRDS and denuders agreed well, much
315 of the useful temporal variability were lost in the time-integrated denuder data (Figure 2b). For
316 example, from 19:00 April 5 to 01:00 April 6 the CRDS measured mixing ratios between 91 and
317 598 pptv. This rapid change of mixing ratios is not captured by the 24-hour average denuder-
318 measured mixing ratio of 348 pptv. The fast time response of the CRDS also captured other rapidly
319 changing HCl features such as the peak observed on between 00:00–06:00 on April 7. The 6-hour
320 event started at 80 pptv and increased at a rate of $1.2 \text{ pptv min}^{-1}$ to 230 pptv over ~120 minutes,
321 followed by a decrease at a rate of $0.5 \text{ pptv min}^{-1}$ for ~240 minutes to 98 pptv. The fast time
322 response of the CRDS on the order of minutes is crucial when applying the technique to the real



323 atmosphere for the purpose of fully constraining the sources and sinks for HCl, for which many
324 precursors have similar lifetimes, and ultimately improve our understanding of the Cl budget
325 (Crisp et al., 2014).

326 Results from the laboratory and ambient intercomparisons were used to determine the
327 accuracy of the HCl analyzer as 5 to 15 %. The lower bound of uncertainty (5 %) was determined
328 from the laboratory intercomparison under the optimal dry conditions (Figure 1). The upper bound
329 of uncertainty (15 %) was consistent across the laboratory intercomparison under the highest RH
330 (80%) conditions tested (Figure 1) and the standard deviation of the orthogonal distance regression
331 slope from the ambient intercomparison (Figure 2a).

332 **3.4 Sampling line and instrument response time assessment**

333 We have thus far demonstrated the efficacy of the CRDS for accurately analyzing gas
334 standards and ambient HCl. However, the potential for sampling losses or desorption sources of
335 surface-active gases that could affect the quality of such measurements is ubiquitous, and the study
336 of these effects are well established (Crisp et al., 2014; Ellis et al., 2010; Pollack et al., 2019;
337 Roscioli et al., 2016). This makes quantification a challenge as there are typically long
338 equilibration times associated with signal stabilization. Long equilibrations make fast time
339 response detection difficult without first characterizing line sorption and desorption, followed by
340 making inlet modifications to minimize losses (Deming et al., 2019; Ellis et al., 2010; Pagonis et
341 al., 2017). To ensure accurate field measurements of HCl, a characterization of the magnitude of
342 HCl loss and desorption during sampling was made. The response time of an instrument to a rapid
343 change in HCl can be calculated by both the time it takes for the measurement to go from zero to
344 100 % of the HCl quantity being delivered, as well as the time it takes to return from the HCl
345 quantity being delivered back to zero.



346 Inlet and instrument surface effects for surface active gases such as HCl can be
347 characterized by fitting decay curves to a double exponential (Ellis et al., 2010; Moravek et al.,
348 2019; Pollack et al., 2019; Zahniser et al., 1995);

$$349 \quad y = y_0 + A_1 e^{\left(\frac{-t-t_0}{\tau_1}\right)} + A_2 e^{\left(\frac{-t-t_0}{\tau_2}\right)} \quad \text{E2}$$

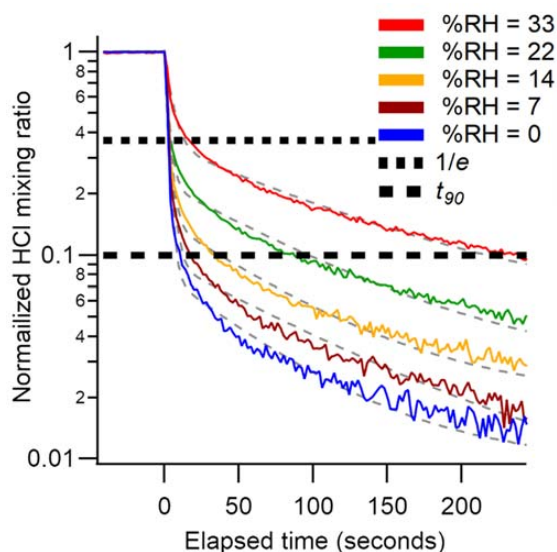
350

351 Where y is the mixing ratio of HCl, y_0 is the mixing ratio at the end of the decay, A_1 and A_2 are
352 proportionality coefficients that determine how much the decay is governed by τ_1 and τ_2
353 respectively, t is the time elapsed, and t_0 is the initial time. The first time constant (τ_1) represents
354 air exchange within the instrument, while the second (τ_2) is the surface interaction equilibrium
355 time between HCl adsorbed to surfaces and the overlying airstream mixing ratio. The only term in
356 this equation that can be optimized for the CRDS is τ_2 , which can be reduced by decreasing the
357 amount of time HCl interacts with inlet surfaces. The sampling flow rate and cavity temperatures
358 are constant for the commercial software and not adjustable, fixing the value of τ_1 . In most reports
359 τ_1 represents the largest change in signal and represents instrument response time. For example,
360 Whitehead et al. (2008) found that τ_1 values governed >75% (i.e. A_1) of changes in measured NH_3 .
361 For the CRDS, measured values of τ_1 were between 5 and 10 seconds under all conditions and
362 could be improved with a faster inlet flowrate for the CRDS to subsample from.

363 An additional set of experiments were undertaken in which a 24 ppbv HCl standard was
364 sampled while varying RH from 0 to 33% (Figure 4). The effect of RH on the response time of the
365 CRDS was measured using a method similar to that described in Section 2.4. The HCl standard
366 gas was sampled over three 10 min pulses at each RH ($\pm 2\%$). The HCl standard was introduced
367 into a 3.17 mm i.d. PFA tube and 10 cm long inlet line. Data was background corrected to levels
368 measured prior to the standard addition calibration and the signal was normalized to the HCl



369 enhancement during the final 10 seconds of each calibration pulse. Due to a lack of inlet
370 characterization for systems measuring HCl, we compare our decay constants to literature values
371 for compounds with similar surface-active properties (e.g. HNO₃ and NH₃). The instrument
372 exchange rate (τ_1) values for spectroscopic methods measuring HNO₃ and NH₃ are generally faster
373 than our measured values for HCl. However, it should be noted that measurements of τ_1 reflect
374 differences in sampling flow rates and internal volume and are likely affected by the internal filters
375 present in the HCl CRDS. Typically, τ_1 was <2 seconds (Ellis et al., 2010; Pollack et al., 2019;
376 Roscioli et al., 2016), but could be as high as 4.5 seconds for larger pulses (1 ppmv) of analyte
377 (Roscioli et al., 2016). We observed a highly variable surface interaction equilibrium time constant
378 (τ_2), with values ranging between 97 and 350 seconds. Reported values of τ_2 for other surface-
379 active gases are similarly variable, with values <50 seconds for heated short clean inlets (Ellis et
380 al., 2010; Pollack et al., 2019; Roscioli et al., 2016), and ~300 seconds for a contaminated inlet
381 measuring NH₃ (Pollack et al., 2019). Major differences in the surface area between our instrument
382 and the instruments we compare here are likely to cause τ_2 discrepancies. Our method employs the
383 use of two HEPA filters that increase the gas to surface interactions by a greater degree.



384

385 **Figure 4.** Background corrected and normalized signal decay curves observed for pulsed HCl (24 ppbv)
386 performed at various RHs. Dashed grey lines represent a double exponential fit to the average of three
387 cycles at each water mixing ratio. The short and long dashed black lines indicate 37 % ($1/e$) and 90 % (t_{90})
388 decrease from the initial signal, respectively.
389

390 Another method for quantifying response time is by calculating the e-folding ($1/e$) signal
391 loss with respect to time. Calculated e-folding response times demonstrated the fast exchange
392 within the system with values comparable to τ_1 . Similarly, a signal decrease of 90% (t_{90}) illustrates
393 the total decay of the sampling line. Using e-folding response time and t_{90} offers a better visual
394 understanding of the relative roles for instrument and inlet responses and the impacts of increasing
395 RH. We summarize the double exponential decay constants, e-folding response time, and t_{90} for
396 the rise and decay of HCl mixing ratios from pulses delivered to the instrument in Table 2 and SI
397 tables 1–4. Increasing the RH increases the response time of the inlet (Figure 4). At the highest
398 experimental RH (33 %), τ_2 is increased by almost a factor of two compared to dry conditions,
399 from seconds to minutes. At lower mixing ratios the higher RH increased the response times to a
400 greater extent (Table 2 and Tables S1–S4). The increased response time at high ambient RH would



401 not compromise stationary measurements in which HCl mixing ratios changed on time scales of
402 minutes to hours but would not capture more rapid changes. The largest impact on CRDS time
403 response likely comes from unavoidable effects of partitioning on the large surface area of the
404 HEPA filters located before the optical cavity. Minimizing inlet effects for the CRDS where
405 observation of HCl mixing ratio changes over <1 min is required (e.g. aircraft or mobile
406 measurements) are most important. The wall interactions of HCl can be reduced by increasing the
407 inlet flow rate and/or decreasing the tubing length (Pagonis et al., 2017).

408 Physical approaches to improving inlet response include inlet material substitution,
409 heating, and pressure reduction, to reduce adsorption of surface-active analytes through removal
410 of surface water and promoted mass transfer of analytes to the gas phase (Sintermann et al., 2011).
411 Deming et. al. (2019) found that PFA tubing had the lowest delay times for semivolatile
412 compounds and would likely extend to small polar molecules like HCl. For a clean thermally-
413 equilibrated inlet, HCl artifacts can be minimized, but if semivolatile aerosol chloride is sampled
414 (e.g. NH_4Cl), the thermodynamic equilibrium can be shifted to result in a positive bias in the HCl
415 measurement, equivalent to similar considerations when measuring HNO_3 and NH_3 (Ellis et al.,
416 2010; Sintermann et al., 2011; Whitehead et al., 2008). While HEPA filters prevent aerosol from
417 entering the cavity, their elevated temperature (45 °C) could lead to volatilization bias and
418 therefore the use of an inlet filter held at ambient temperature to reduce such effects is
419 recommended at a minimum.

420 Chemical approaches can also help mitigate adsorption of surface-active molecules to inlet
421 surfaces through derivatization or passivation. The silanization of glass to form an inert fluorinated
422 or silicon coating on a virtual impactor or the introduction of a gaseous fluorinated compound that
423 adsorbs competitively to instrument surfaces in place of the analytes have been demonstrated to



424 substantially reduce surface adsorption on PFA (Ellis et al., 2010; Moravek et al., 2019; Pollack
 425 et al., 2019; Roscioli et al., 2016; Wilkerson et al., 2021). However, environmental impacts must
 426 be considered when constantly adding fluorinated compounds to sampling flows as they may have
 427 deleterious environmental consequences (Cousins et al., 2020). In particular,
 428 perfluorobutanesulfonic acid, the fluorinated chemical suggested for passivating inlets (Roscioli
 429 et al., 2016), is subject to usage restrictions in some European countries (ECHA, 2020) based on
 430 potential negative human and environmental health impacts (Benskin et al., 2012; Sunderland et
 431 al., 2019). The high surface activity of perfluorobutanesulfonic acid is likely to cause issues in the
 432 analyzer used in this work because the gas sample comes into direct contact with the high
 433 reflectivity mirrors. Acid deposition onto mirrors will degrade their reflectivity.

434
 435 **Table 2.** Summary of the fit parameters for the double exponential decay curves as a
 436 function of mixing ratio and humidity, e-folding response time, and t_{90} .
 437

Mixing ratio (ppbv)	Residence time (seconds)	RH (%)	τ_1 (seconds)	τ_2 (seconds)	$1/e$ (seconds)	t_{90} (seconds)
12	0.021	0	10.3	123	26.5	101
16	0.028	0	9.6	200	24.7	82
21	0.037	0	10.1	300	26.4	74
		0	2.7	97	2.5	10
		7	5.0	124	2.5	18
		14	5.0	114	2.5	32
24	–	22	5.0	123	3.9	86
		33	10.0	189	16.1	239
		0	9.4	188	24.5	62
32	0.056	0	9.4	188	24.5	62
45	0.079	0	9.7	350	25.6	54

438

439

440 4. Conclusions

441 The suitability of a CRDS analyzer for measuring ambient atmospheric HCl were explored
 442 through calibration, inlet and analyzer sampling challenges, and intercomparison to established



443 atmospheric sampling techniques for strong acids. In comparison to other reported
444 instrumentation, the CRDS is shown performing similar or better than the most sensitive HCl
445 measurements reported. As with many in situ measurements of HCl, the most significant limitation
446 is adsorption/desorption loss and release on inlet surfaces, with the deposition effects increasing
447 with increasing RH and decreasing HCl mixing ratios. Given the longstanding knowledge of these
448 issues for surface active gases, such as HNO₃ and NH₃, there are a variety of chemical and physical
449 options, discussed in this study, to mitigate inlet effects and achieve faster response times for the
450 CRDS. Increasing the flowrate of the sampling inlet, while maintaining laminar flow, is the
451 simplest approach to reducing surface effects discussed in Section 3.4. Spectra capturing errors in
452 the measurement of HCl for the CRDS can occur at high levels of VOCs (e.g. near emission point
453 sources or biomass burning plumes) or instrument instabilities (e.g. pressure fluctuations),
454 however potential instrument errors are minimal under most operating and atmospheric conditions.
455 Finally, comparison with annular denuder observations agreed within the combined uncertainties,
456 with the CRDS measurement rate demonstrating the power of capturing transient events that are
457 important to constraining atmospheric chlorine chemistry (e.g. photolysis of precursors,
458 thermodynamic partitioning, and direct emissions).

459 **Author Contributions**

460 TCF, PRV, and KERD collected and analyzed the data. TCF, PRV, JAN, SSB, TCV, and CJY
461 conceived of and designed the experiments. Funding was obtained by CJY. The manuscript was
462 written by TCF with input from all authors.

463 **Competing Interests**

464 The authors declare that they have no conflict of interest.



465 Acknowledgements

466 We acknowledge the Natural Sciences Engineering and Research Council of Canada and York
467 University for funding. We thank Andrea Angelucci and Sonya Daljeet for assistance with data
468 collection.

469 References

- 470 Benskin, J. P., Muir, D. C. G., Scott, B. F., Spencer, C., De Silva, A. O., Kylin, H., Martin, J. W.,
471 Morris, A., Lohmann, R., Tomy, G., Rosenberg, B., Taniyasu, S. and Yamashita, N.:
472 Perfluoroalkyl Acids in the Atlantic and Canadian Arctic Oceans, *Environ. Sci. Technol.*, 46(11),
473 5815–5823, doi:10.1021/es300578x, 2012.
- 474 Bondy, A. L., Wang, B., Laskin, A., Craig, R. L., Nhliziyo, M. V, Bertman, S. B., Pratt, K. A.,
475 Shepson, P. B. and Ault, A. P.: Inland Sea Spray Aerosol Transport and Incomplete Chloride
476 Depletion: Varying Degrees of Reactive Processing Observed during SOAS, *Environ. Sci.*
477 *Technol.*, (51), 9533–9542, doi:10.1021/acs.est.7b02085, 2017.
- 478 Butz, A., Dinger, A. S., Bobrowski, N., Kostinek, J., Fieber, L., Fischerkeller, C., Giuffrida, G.
479 B., Hase, F., Klappenbach, F., Kuhn, J., Lübcke, P., Tirpitz, L. and Tu, Q.: Remote sensing of
480 volcanic CO₂, HF, HCl, SO₂, and BrO in the downwind plume of Mt. Etna, *Atmos. Meas.*
481 *Tech.*, 10(1), 1–14, doi:10.5194/amt-10-1-2017, 2017.
- 482 Clegg, S. L. and Brimblecombe, P.: Potential degassing of hydrogen chloride from acidified
483 sodium chloride droplets, *Atmos. Environ.*, 19(3), 465–470, doi:https://doi.org/10.1016/0004-
484 6981(85)90167-2, 1985.
- 485 Cousins, I. T., DeWitt, J. C., Gluege, J., Goldenman, G., Herzke, D., Lohmann, R., Ng, C.,
486 Scheringer, M. and Wang, Z.: The high persistence of PFAS is sufficient for their management
487 as a chemical class, *Environ. Sci. Process. Impacts*, doi:10.1039/D0EM00355G, 2020.
- 488 Crisp, T. A, Lerner, B. M., Williams, E. J., Quinn, P. K., Bates, T. S. and Bertram, T. H.:
489 Observations of gas phase hydrochloric acid in the polluted marine boundary layer, *J. Geophys.*
490 *Res. Atmos.*, 6897–6915, doi:10.1002/2013JD020992, 2014.
- 491 Crosson, E. R.: A cavity ring-down analyzer for measuring atmospheric levels of methane,
492 carbon dioxide, and water vapor, *Appl. Phys. B*, 92(3), 403–408, doi:10.1007/s00340-008-3135-
493 y, 2008.
- 494 Dawe, K. E. R., Furlani, T. C., Kowal, S. F., Kahan, T. F., Vandenboer, T. C. and Young, C. J.:
495 Formation and emission of hydrogen chloride in indoor air, *Indoor Air*, 70–78,
496 doi:10.1111/ina.12509, 2019.
- 497 Deming, B. L., Pagonis, D., Liu, X., Day, D. A., Talukdar, R., Krechmer, J. E., Gouw, J. A. De,
498 Jimenez, J. L. and Ziemann, P. J.: Measurements of delays of gas-phase compounds in a wide
499 variety of tubing materials due to gas – wall interactions, *Atmos. Meas. Tech.*, 12, 3453–3461,
500 doi: 10.5194/amt-12-3453-2019, 2019.



- 501 ECHA: Four new substances added to Candidate List, [online] Available from:
502 <https://www.echa.europa.eu/-/four-new-substances-added-to-candidate-list> (Accessed 30 June
503 2020), 2020.
- 504 Eisele, F. L. and Tanner, D. J.: Measurement of the gas phase concentration of H₂SO₄ and
505 methane sulfonic acid and estimates of H₂SO₄ production and loss in the atmosphere, J.
506 Geophys. Res. Atmos., 98(D5), 9001–9010, doi:10.1029/93JD00031, 1993.
- 507 Ellis, R. A., Murphy, J. G., Pattey, E., Haarlem, R. Van and Brien, J. M. O.: Characterizing a
508 Quantum Cascade Tunable Infrared Laser Differential Absorption Spectrometer (QC-TILDAS)
509 for measurements of atmospheric ammonia, Atmos. Meas. Tech., 3309–3338, doi: 10.5194/amt-
510 3-397-2010, 2010.
- 511 Finlayson-Pitts, B. J., Ezell, M. J. and Pitts, J. N.: Formation of chemically active chlorine
512 compounds by reactions of atmospheric NaCl particles with gaseous N₂O₅ and ClONO₂,
513 Nature, 337(6204), 241–244, doi:10.1038/337241a0, 1989.
- 514 Gard, E. E., Kleeman, M. J., Gross, D. S., Hughes, L. S., Allen, J. O., Morrical, B. D.,
515 Fergenson, D. P., Dienes, T., Ga, M. E., Johnson, R. J., Cass, G. R. and Prather, K. A.: Direct
516 Observation of Heterogeneous Chemistry in the Atmosphere, Science, 279, doi:
517 10.1126/science.279.5354.1184, 1998.
- 518 Gordon, I. E., Rothman, L. S., Hill, C., Kochanov, R. V., Tan, Y., Bernath, P. F., Birk, M.,
519 Boudon, V., Campargue, A., Chance, K. V., Drouin, B. J., Flaud, J.-M., Gamache, R. R., Hodges,
520 J. T., Jacquemart, D., Perevalov, V. I., Perrin, A., Shine, K. P., Smith, M.-A. H., Tennyson, J.,
521 Toon, G. C., Tran, H., Tyuterev, V. G., Barbe, A., Császár, A. G., Devi, V. M., Furtenbacher, T.,
522 Harrison, J. J., Hartmann, J.-M., Jolly, A., Johnson, T. J., Karman, T., Kleiner, I., Kyuberis, A.
523 A., Loos, J., Lyulin, O. M., Massie, S. T., Mikhailenko, S. N., Moazzen-Ahmadi, N., Müller, H.
524 S. P., Naumenko, O. V., Nikitin, A. V., Polyansky, O. L., Rey, M., Rotger, M., Sharpe, S. W.,
525 Sung, K., Starikova, E., Tashkun, S. A., Auwera, J. Vander, Wagner, G., Wilzewski, J., Wcisło,
526 P., Yu, S. and Zak, E. J.: The HITRAN2016 molecular spectroscopic database, J. Quant.
527 Spectrosc. Radiat. Transf., 203, 3–69, doi:<https://doi.org/10.1016/j.jqsrt.2017.06.038>, 2017.
- 528 Hagen, C. L., Lee, B. C., Franka, I. S., Rath, J. L., Vandenboer, T. C., Roberts, J. M., Brown, S.
529 S. and Yalin, A. P.: Cavity ring-down spectroscopy sensor for detection of hydrogen chloride,
530 Atmos. Meas. Tech., 7(2), 345–357, doi:10.5194/amt-7-345-2014, 2014.
- 531 Haskins, J. D., Jaeglé, L., Shah, V., Lee, B. H., Lopez-Hilfiker, F. D., Campuzano-Jost, P.,
532 Schroder, J. C., Day, D. A., Guo, H., Sullivan, A. P., Weber, R., Dibb, J., Campos, T., Jimenez,
533 J. L., Brown, S. S. and Thornton, J. A.: Wintertime Gas-Particle Partitioning and Speciation of
534 Inorganic Chlorine in the Lower Troposphere Over the Northeast United States and Coastal
535 Ocean, J. Geophys. Res. Atmos., 123(22), 12,812–897,916, doi:10.1029/2018JD028786, 2018.
- 536 Huey, L. G., Villalta, P. W., Dunlea, E. J., Hanson, D. R. and Howard, C. J.: Reactions of CF₃O-
537 with Atmospheric Trace Gases, J. Phys. Chem., 100(1), 190–194, doi:10.1021/jp951928u, 1996.
- 538 Jurkat, T., Voigt, C., Arnold, F., Schlager, H., Aufmhoff, H., Schmale, J., Schneider, J.,
539 Lichtenstern, M. and Dörnbrack, A.: Airborne stratospheric ITCIMS measurements of SO₂, HCl,
540 and HNO₃ in the aged plume of volcano Kasatochi, J. Geophys. Res. Atmos., 115(D2),
541 doi:<https://doi.org/10.1029/2010JD013890>, 2010.



- 542 Karellas, N. S., Chen, Q. F., De Brou, G. B. and Milburn, R. K.: Real time air monitoring of
543 hydrogen chloride and chlorine gas during a chemical fire, *J. Hazard. Mater.*, 102(1), 105–120,
544 doi:[https://doi.org/10.1016/S0304-3894\(03\)00205-X](https://doi.org/10.1016/S0304-3894(03)00205-X), 2003.
- 545 Keene, W. C., Khalil, M. A. K., Erickson, D. J., McCulloch, A., Graedel, T. E., Lobert, J. M.,
546 Aucott, M. L., Gong, S. L., Harper, D. B., Kleiman, G., Midgley, P., Moore, R. M., Seuzaret, C.,
547 Sturges, W. T., Benkovitz, C. M., Koropalov, V., Barrie, L. A. and Li, Y. F.: Composite global
548 emissions of reactive chlorine from anthropogenic and natural sources: Reactive Chlorine
549 Emissions Inventory, *J. Geophys. Res. Atmos.*, 104(D7), 8429–8440,
550 doi:[10.1029/1998JD100084](https://doi.org/10.1029/1998JD100084), 1999.
- 551 Keene, W. C., Stutz, J., Pszenny, A. A. P., Maben, J. R., Fischer, E. V, Smith, A. M., von
552 Glasow, R., Pechtl, S., Sive, B. C. and Varner, R. K.: Inorganic chlorine and bromine in coastal
553 New England air during summer, *J. Geophys. Res. Atmos.*, 112(D10),
554 doi:[10.1029/2006JD007689](https://doi.org/10.1029/2006JD007689), 2007.
- 555 Keene, W. C., Long, M. S., Pszenny, A. A. P., Sander, R., Maben, J. R., Wall, A. J., O’Halloran,
556 T. L., Kerkweg, A., Fischer, E. V and Schrems, O.: Latitudinal variation in the multiphase
557 chemical processing of inorganic halogens and related species over the eastern North and South
558 Atlantic Oceans, *Atmos. Chem. Phys.*, 9(19), 7361–7385, doi:[10.5194/acp-9-7361-2009](https://doi.org/10.5194/acp-9-7361-2009), 2009.
- 559 Kim, S., Huey, L. G., Stickel, R. E., Pierce, R. B., Chen, G., Avery, M. A., Dibb, J. E., Diskin,
560 G. S., Sachse, G. W., McNaughton, C. S., Clarke, A. D., Anderson, B. E. and Blake, D. R.:
561 Airborne measurements of HCl from the marine boundary layer to the lower stratosphere over
562 the North Pacific Ocean during INTEX-B, *Atmos. Chem. Phys. Discuss.*, 2008, 3563–3595,
563 doi:[10.5194/acpd-8-3563-2008](https://doi.org/10.5194/acpd-8-3563-2008), 2008.
- 564 Kochanov, R. V, Gordon, I. E., Rothman, L. S., Shine, K. P., Sharpe, S. W., Johnson, T. J.,
565 Wallington, T. J., Harrison, J. J., Bernath, P. F., Birk, M., Wagner, G., Le Bris, K., Bravo, I. and
566 Hill, C.: Infrared absorption cross-sections in HITRAN2016 and beyond: Expansion for climate,
567 environment, and atmospheric applications, *J. Quant. Spectrosc. Radiat. Transf.*, 230, 172–221,
568 doi:<https://doi.org/10.1016/j.jqsrt.2019.04.001>, 2019.
- 569 Lao, M., Crilley, L. R., Salehpoor, L., Furlani, T. C., Bourgeois, I., Neuman, J. A., Rollins, A.
570 W., Veres, P. R., Washenfelder, R. A., Womack, C. C., Young, C. J. and VandenBoer, T. C.: A
571 portable, robust, stable and tunable calibration source for gas-phase nitrous acid (HONO),
572 *Atmos. Meas. Tech.*, 2020, 13, 5873–5890, doi:[10.5194/amt-13-5873-2020](https://doi.org/10.5194/amt-13-5873-2020), 2020.
- 573 Lee, B. H., Lopez-Hilfiker, F. D., Schroder, J. C., Campuzano-Jost, P., Jimenez, J. L., McDuffie,
574 E. E., Fibiger, D. L., Veres, P. R., Brown, S. S., Campos, T. L., Weinheimer, A. J., Flocke, F. F.,
575 Norris, G., O’Mara, K., Green, J. R., Fiddler, M. N., Bililign, S., Shah, V., Jaeglé, L. and
576 Thornton, J. A.: Airborne Observations of Reactive Inorganic Chlorine and Bromine Species in
577 the Exhaust of Coal-Fired Power Plants, *J. Geophys. Res. Atmos.*, 123(19), 11,225–11,237,
578 doi:[10.1029/2018JD029284](https://doi.org/10.1029/2018JD029284), 2018.
- 579 Ma, Y., He, Y., Yu, X., Chen, C., Sun, R. and Tittel, F. K.: HCl ppb-level detection based on
580 QEPAS sensor using a low resonance frequency quartz tuning fork, *Sensors Actuators, B Chem.*,
581 233, 388–393, doi:[10.1016/j.snb.2016.04.114](https://doi.org/10.1016/j.snb.2016.04.114), 2016.
- 582 MacInnis, J. J., VandenBoer, T. C. and Young, C. J.: Development of a gas phase source for



- 583 perfluoroalkyl acids to examine atmospheric sampling methods, *Analyst*, 141(12), 3765–3775,
584 doi:10.1039/C6AN00313C, 2016.
- 585 Marcy, T. P., Fahey, D. W., Gao, R. S., Popp, P. J., Richard, E. C., Thompson, T. L., Rosenlof,
586 K. H., Ray, E. A., Salawitch, R. J., Atherton, C. S., Bergmann, D. J., Ridley, B. A., Weinheimer,
587 A. J., Loewenstein, M., Weinstock, E. M. and Mahoney, M. J.: Quantifying Stratospheric Ozone
588 in the Upper Troposphere with in Situ Measurements of HCl, *Science*, 304(5668), 261 LP – 265,
589 doi:10.1126/science.1093418, 2004.
- 590 Mattila, J. M., Lakey, P. S. J., Shiraiwa, M., Wang, C., Abbatt, J. P. D., Arata, C., Goldstein, A.
591 H., Ampollini, L., Katz, E. F., DeCarlo, P. F., Zhou, S., Kahan, T. F., Cardoso-Saldaña, F. J.,
592 Ruiz, L. H., Abeleira, A., Boedicker, E. K., Vance, M. E. and Farmer, D. K.: Multiphase
593 Chemistry Controls Inorganic Chlorinated and Nitrogenated Compounds in Indoor Air during
594 Bleach Cleaning, *Environ. Sci. Technol.*, 54(3), 1730–1739, doi:10.1021/acs.est.9b05767, 2020.
- 595 Moravek, A., Singh, S., Pattey, E., Pelletier, L. and Murphy, J.: Measurements and quality
596 control of ammonia eddy covariance fluxes: a new strategy for high-frequency attenuation
597 correction, *Atmos. Meas. Tech.*, 12, 6059–6078, doi:10.5194/amt-12-6059-2019, 2019.
- 598 Neuman, J. A., Huey, L. G., Ryerson, T. B. and Fahey, D. W.: Study of Inlet Materials for
599 Sampling Atmospheric Nitric Acid, *Environ. Sci. Technol.*, 33(7), 1133–1136,
600 doi:10.1021/es980767f, 1999.
- 601 Osthoff, H. D., Roberts, J. M., Ravishankara, A. R., Williams, E. J., Lerner, B. M., Sommariva,
602 R., Bates, T. S., Coffman, D., Quinn, P. K., Dibb, J. E., Stark, H., Burkholder, J. B., Talukdar, R.
603 K., Meagher, J., Fehsenfeld, F. C. and Brown, S. S.: High levels of nitryl chloride in the polluted
604 subtropical marine boundary layer, *Nat. Geosci*, 1(5), 324–328, 2008.
- 605 Pagonis, D., Krechmer, J. E., de Gouw, J., Jimenez, J. L. and Ziemann, P. J.: Effects of gas–wall
606 partitioning in Teflon tubing and instrumentation on time-resolved measurements of gas-phase
607 organic compounds, *Atmos. Meas. Tech.*, 10(12), 4687–4696, doi:10.5194/amt-10-4687-2017,
608 2017.
- 609 Place, B. K., Young, C. J., Ziegler, S. E., Edwards, K. A., Salehpoor, L. and VandenBoer, T. C.:
610 Passive sampling capabilities for ultra-trace quantitation of atmospheric nitric acid (HNO₃) in
611 remote environments, *Atmos. Environ.*, 191, 360–369, doi:10.1016/j.atmosenv.2018.08.030,
612 2018.
- 613 Pollack, I. B., Lindaas, J., Roscioli, J. R., Agnese, M., Permar, W., Hu, L. and Fischer, E. V:
614 Evaluation of ambient ammonia measurements from a research aircraft using a closed-path QC-
615 TILDAS operated with active continuous passivation, *Atmos. Meas. Tech.*, 12(7), 3717–3742,
616 doi:10.5194/amt-12-3717-2019, 2019.
- 617 Pszenny, A. A. P., Keene, W. C., Jacob, D. J., Fan, S., Maben, J. R., Zetwo, M. P., Springer-
618 Young, M. and Galloway, J. N.: Evidence of inorganic chlorine gases other than hydrogen
619 chloride in marine surface air, *Geophys. Res. Lett.*, 20(8), 699–702, doi:10.1029/93GL00047,
620 1993.
- 621 Roberts, J. M., Osthoff, H. D., Brown, S. S. and Ravishankara, A. R.: N₂O₅ Oxidizes Chloride
622 to Cl₂ in Acidic Atmospheric Aerosol, *Science*, 321(5892), 1059–1059,
623 doi:10.1126/science.1158777, 2008.



- 624 Roscioli, J. R., Zahniser, M. S., Nelson, D. D., Herndon, S. C. and Kolb, C. E.: New Approaches
625 to Measuring Sticky Molecules: Improvement of Instrumental Response Times Using Active
626 Passivation, *J. Phys. Chem. A*, 120(9), 1347–1357, doi:10.1021/acs.jpca.5b04395, 2016.
- 627 Sherwen, T., Schmidt, J. A., Evans, M. J., Carpenter, L. J., Großmann, K., Eastham, S. D., Jacob,
628 D. J., Dix, B., Koenig, T. K., Sinreich, R., Ortega, I., Volkamer, R., Saiz-Lopez, A., Prados-
629 Roman, C., Mahajan, A. S. and Ordóñez, C.: Global impacts of tropospheric halogens (Cl, Br, I)
630 on oxidants and composition in GEOS-Chem, *Atmos. Chem. Phys.*, 16(18), 12239–12271,
631 doi:10.5194/acp-16-12239-2016, 2016.
- 632 Simpson, W. R., Glasow, R. Von, Riedel, K., Anderson, P., Ariya, P., Bottenheim, J., Burrows,
633 J. and Carpenter, L. J.: Halogens and their role in polar boundary-layer ozone depletion, *Atmos.*
634 *Chem. Phys.*, 4375–4418, doi: 10.5194/acp-7-4375-2007, 2007.
- 635 Simpson, W. R., Brown, S. S., Saiz-Lopez, A., Thornton, J. A. and Von Glasow, R.:
636 Tropospheric Halogen Chemistry: Sources, Cycling, and Impacts, *Chem. Rev.*, 115(10), 4035–
637 4062, doi:10.1021/cr5006638, 2015.
- 638 Sintermann, J., Spirig, C., Jordan, A., Kuhn, U., Ammann, C. and Neftel, A.: Eddy covariance
639 flux measurements of ammonia by high temperature chemical ionisation mass spectrometry,
640 *Atmos. Meas. Tech.*, 4(3), 599–616, doi:10.5194/amt-4-599-2011, 2011.
- 641 Solomon, S.: Stratospheric ozone depletion: A review of concepts and history, *Rev. Geophys.*,
642 37(3), 275–316, doi:10.1029/1999RG900008, 1999.
- 643 Sunderland, E. M., Hu, X. C., Dassuncao, C., Tokranov, A. K., Wagner, C. C. and Allen, J. G.:
644 A review of the pathways of human exposure to poly- and perfluoroalkyl substances (PFASs)
645 and present understanding of health effects, *J. Expo. Sci. Environ. Epidemiol.*, 29(2), 131–147,
646 doi:10.1038/s41370-018-0094-1, 2019.
- 647 Thaler, R. D., Mielke, L. H. and Osthoff, H. D.: Quantification of Nitryl Chloride at Part Per
648 Trillion Mixing Ratios by Thermal Dissociation Cavity Ring-Down Spectroscopy, *Anal. Chem.*,
649 83(7), 2761–2766, doi:10.1021/ac200055z, 2011.
- 650 Thornton, J. A., Kercher, J. P., Riedel, T. P., Wagner, N. L., Cozic, J., Holloway, J. S., Dubé, W.
651 P., Wolfe, G. M., Quinn, P. K., Middlebrook, A. M., Alexander, B. and Brown, S. S.: A large
652 atomic chlorine source inferred from mid-continental reactive nitrogen chemistry, *Nature*, 464,
653 271, doi:10.1038/nature08905, 2010.
- 654 United States Environmental Protection Agency: Compendium of Methods for the Determination
655 of Inorganic Compounds in Ambient Air: Determination of reactive acidic and basic gases and
656 strong acidity of atmospheric fine particles (<2.5 μm) (Compendium Method IO-4.2), 1999.
- 657 Valach, R.: The origin of the gaseous form of natural atmospheric chlorine, *Tellus Ser. B Chem.*
658 *Phys. Meteorol.*, 1967.
- 659 Veres, P., Roberts, J. M., Warneke, C., Welsh-Bon, D., Zahniser, M., Herndon, S., Fall, R. and
660 de Gouw, J.: Development of negative-ion proton-transfer chemical-ionization mass
661 spectrometry (NI-PT-CIMS) for the measurement of gas-phase organic acids in the atmosphere,
662 *Int. J. Mass Spectrom.*, 274(1–3), 48–55, doi:10.1016/j.ijms.2008.04.032, 2008.
- 663 Voss, P. B., Stimpfle, R. M., Cohen, R. C., Hanisco, T. F., Bonne, G. P., Perkins, K. K.,



- 664 Lanzendorf, E. J., Anderson, J. G., Salawitch, R. J., Webster, C. R., Scott, D. C., May, R. D.,
665 Wennberg, P. O., Newman, P. A., Lait, L. R., Elkins, J. W. and Bui, T. P.: Inorganic chlorine
666 partitioning in the summer lower stratosphere: Modeled and measured [ClONO₂]/[HCl] during
667 POLARIS, *J. Geophys. Res. Atmos.*, 106(D2), 1713–1732,
668 doi:<https://doi.org/10.1029/2000JD900494>, 2001.
- 669 Wang, X., Jacob, D. J., Eastham, S. D., Sulprizio, M. P., Zhu, L., Chen, Q., Alexander, B.,
670 Sherwen, T., Evans, M. J., Lee, B. H., Haskins, J. D., Lopez-hilfiker, F. D., Thornton, J. A.,
671 Huey, G. L. and Liao, H.: The role of chlorine in global tropospheric chemistry, *Atmos. Chem.*
672 *Phys.*, 3981–4003, doi: 10.5194/acp-19-3981-2019, 2019.
- 673 Webster, C. R., May, R. D., Trimble, C. A., Chave, R. G. and Kendall, J.: Aircraft (ER-2) laser
674 infrared absorption spectrometer (ALIAS) for in-situ stratospheric measurements of HCl, N₂O,
675 CH₄, NO₂, and HNO₃, *Appl. Opt.*, 33(3), 454–472, doi:10.1364/AO.33.000454, 1994.
- 676 Whitehead, J. D., Twigg, M., Famulari, D., Nemitz, E., Sutton, M. A., Gallagher, M. W. and
677 Fowler, D.: Evaluation of Laser Absorption Spectroscopic Techniques for Eddy Covariance Flux
678 Measurements of Ammonia, *Environ. Sci. Technol.*, 42(6), 2041–2046, doi:10.1021/es071596u,
679 2008.
- 680 Wilkerson, J., Sayres, D. S., Smith, J. B., Allen, N., Rivero, M., Greenberg, M., Martin, T. and
681 Anderson, J. G.: In situ observations of stratospheric HCl using three-mirror integrated cavity
682 output spectroscopy, *Atmos. Meas. Tech. Discuss.*, 2021, 1–38, doi:10.5194/amt-2021-6, 2021.
- 683 Young, A. H., Keene, W. C., Pszenny, A. A. P., Sander, R., Thornton, J. A., Riedel, T. P. and
684 Maben, J. R.: Phase partitioning of soluble trace gases with size-resolved aerosols in near-surface
685 continental air over northern Colorado, USA, during winter, *J. Geophys. Res. Atmos.*, 118(16),
686 9414–9427, doi:10.1002/jgrd.50655, 2013.
- 687 Young, C. J., Washenfelder, R. A., Roberts, J. M., Mielke, L. H., Osthoff, H. D., Tsai, C.,
688 Pikel'naya, O., Stutz, J., Veres, P. R., Cochran, A. K., VandenBoer, T. C., Flynn, J., Grossberg,
689 N., Haman, C. L., Lefer, B., Stark, H., Graus, M., de Gouw, J., Gilman, J. B., Kuster, W. C. and
690 Brown, S. S.: Vertically Resolved Measurements of Nighttime Radical Reservoirs in Los
691 Angeles and Their Contribution to the Urban Radical Budget, *Environ. Sci. Technol.*, 46(20),
692 10965–10973, doi:10.1021/es302206a, 2012.
- 693 Young, C. J., Washenfelder, R. A., Edwards, P. M., Parrish, D. D., Gilman, J. B., Kuster, W. C.,
694 Mielke, L. H., Osthoff, H. D., Tsai, C., Pikel'naya, O., Stutz, J., Veres, P. R., Roberts, J. M.,
695 Griffith, S., Dusanter, S., Stevens, P. S., Flynn, J., Grossberg, N., Lefer, B., Holloway, J. S.,
696 Peischl, J., Ryerson, T. B., Atlas, E. L., Blake, D. R. and Brown, S. S.: Chlorine as a primary
697 radical: Evaluation of methods to understand its role in initiation of oxidative cycles, *Atmos.*
698 *Chem. Phys.*, 14(7), 3427–3440, doi:10.5194/acp-14-3427-2014, 2014.
- 699 Young, C. J., Zhou, S., Siegel, J. A. and Kahan, T. F.: Illuminating the dark side of indoor
700 oxidants, *Environ. Sci. Process. Impacts*, 21(8), 1229–1239, doi:10.1039/C9EM00111E, 2019.
- 701 Zahniser, M. S., Nelson, D. D., McManus, B., Kebabian, P. L., Lloyd, D., Fowler, D., Jenkinson,
702 D. S., Monteith, J. L. and Unsworth, M. H.: Measurement of trace gas fluxes using tunable diode
703 laser spectroscopy, *Philos. Trans. R. Soc. London. Ser. A Phys. Eng. Sci.*, 351(1696), 371–382,
704 doi:10.1098/rsta.1995.0040, 1995.